Model Order Reduction of Linear Peridynamic Systems
Using Static Condensation

Yakubu Kasimu Galadima, Erkan Oterkus* and Selda Oterkus

PeriDynamics Research Centre, Department of Naval Architecture, Ocean and Marine Engineering

University of Strathclyde, Glasgow, UK

Abstract: Static condensation is widely used as a model order reduction technique to lower the computational effort and complexity of classical continuum based computational models such as the Finite Element models. Peridynamic theory is a nonlocal theory developed primarily to overcome the shortcoming of the classical continuum-based models in handling discontinuous system response. In this study, a model order reduction algorithm is developed based on the static condensation technique to reduce the order of peridynamic models. Numerical examples are considered to demonstrate the robustness of the proposed reduction algorithm in reproducing the static, dynamic and eigenresponse of the full peridynamic models.

Keywords: Peridynamic theory; Classical continuum theory; Finite Element models; Static condensation

1.0 Introduction

The increasing requirement for cost saving means more complex and increasingly larger systems needed to be mathematically modelled and simulated, thus increasing computational time and cost. In order to ensure computational efficiency, various techniques have been developed to reduce the size of the model to be solved for either static or dynamic responses.

Every mathematical model is an attempt to imitate a physical process. Because of the uncertainties involved in the parameters that describe the system such as loads and material properties, inaccuracies are inevitably introduced into the model and ultimately to the predicted response of the system. In the design of high technology systems, the accuracy of the mathematical model is crucial because the margin for errors for such systems is usually much less than for conventional systems. It therefore becomes necessary to verify results obtained from virtual simulation with experimental results.

Traditionally, Finite Element (FE) Models are used to predict the static and dynamic responses of structural systems across a wide spectrum of industries such as Aerospace, Automobile and Civil Engineering. Where the mathematically predicted dynamic response of the system needs to be verified experimentally, a structural dynamic test is conducted on a physical model. Usually the dynamic experiment is conducted with fewer degrees of freedom (DoFs) than the mathematical model. This

Corresponding author: Erkan Oterkus, University of Strathclyde, PeriDynamics Research Centre, Glasgow G4 0LZ, United Kingdom, E-mail: erkan.oterkus@strath.ac.uk

represents a classic motivation to develop model reduction techniques the objective of which is to allow for correlation of dynamic response from experiment with that of the mathematical model by reducing the DoFs of the FE model in order to eliminate the problem of mesh incompatibility. The reduced mathematical model in this sense is called Test Analysis Model (TAM) [1]]. Several techniques have been proposed to help with the condensation of static and dynamic FE models [2-7].

Despite its many successes, there are still numerous problems for which the FE method based on the classical continuum model is simply inadequate. One factor responsible for the inadequacy is the fact that the governing equations describing the response of systems in the classical continuum theory rely on spatial derivatives. Such partial derivatives by their nature are not valid in the presence of discontinuous system response such as cracks.

Peridynamic theory was developed [8] primarily to overcome the shortcomings of the classical continuum mechanics in handling discontinuous system response. Built on a mathematical framework based on an integro-differential framework, the development of Peridynamic (PD) theory paved the way for the unification of the mathematical modelling of continuous media, fracture and particles in a single modelling framework which can find application in situations involving evolution and propagation of discontinuities such as crack nucleation and growth using the same field equation as in the continuous case. Another feature of the PD formulation is that it is a nonlocal theory that incorporate the concept of long-range force by allowing interaction of particles located at finite distance from each other through a pairwise force field.

Since its introduction [8], the PD theory has been successfully deployed to study a range of engineering systems [9-15]. However, the use of PD theory in solving practical engineering problem implies dealing with systems with very large DoFs. This comes with the attendant consequence of high computational cost. In response, several multiscale techniques have been proposed to achieve the goal of reducing complexity of PD models. An adaptive refinement and multiscale algorithm was developed in [16] which essentially allowed use of variable horizon size in different regions of a peridynamic model to gain computational efficiency.

A hierarchical multiscale modelling framework that coupled Molecular Dynamics (MD) with Peridynamics (PD) was developed in [17]. The coupling of PD particles at coarse scale and the fine scale MD particles was achieved through an intermediate mesoscale region called the coarse-grain atomic model. The algorithm so developed was a hierarchical downscaling framework that allowed information about the system at the PD macro scale to be transferred and captured at the MD microscale.

A coarsening method for linear Peridynamics was proposed and implemented for one-dimension in [18] and was extend in [19] for two dimensional applications. The objective of the coarsening algorithm was to derive a simplified model from a detailed and more complex model by retaining fewer DoFs on one hand and preserving the effect of the excluded DoFs in the response of the model on the other hand.

Numerical investigation conducted in both works demonstrated the robustness of the technique in reducing the order of PD model for a range of problems without compromising on predictive capability.

A key limitation of the coarsening algorithm is the fact that the boundary data must be specified on the retained DoFs. In other words, applied body force or prescribed nonzero displacement must be specified on the retained DoFs. This consequently places restrictions on which DoFs to eliminate and which to retain. Another limitation of the coarsening method is that the algorithm is not suitable for application in solving dynamic equilibrium problems.

The objective in this work is to present a model order reduction algorithm based on static condensation method [2] that is similar to the coarsening methodology [18] described above in that both methodologies seek to reduce the complexity of a PD model and hence computational effort by reducing the DoFs of the model and yet still able to accurately predict the response of the system. However, the proposed algorithm in this work promises to have extended capabilities covering both static and dynamic system response. Numerical investigation will be conducted to demonstrate the robustness of the algorithm in effectively reducing the order of PD models for static, dynamic and modal response.

In what will follow, a brief overview of the PD theory will be given in section 3 while the algorithm and procedure of statically condensing a PD model will be laid out in section 4. In section 3.1, the expression for static condensation of PD static response problem will be derived, to be followed in section 3.2 with the derivation of the expression for the static condensation of PD dynamic response analysis. In section 3.3, the modal equations of PD theory will be derived, and the proposed condensation algorithm will be applied to obtain the reduced order model for PD eigenproblem. The general form of the reduced micromodulus function is presented in section 4.0. Numerical demonstration of the capabilities of the proposed reduction algorithm in reproducing the static, dynamic and modal response of PD model using fewer DoFs is presented in section 5.0.

2.0 Peridynamic theory

Recalling from the classical continuum theory, the equation of motion of a medium arising from conservation of momentum is as follows:

$$\rho(x)\ddot{u}(x,t) = \nabla \cdot \sigma + b(x,t) \tag{1}$$

where ρ is the mass density of the medium, σ is the stress tensor, b is a vector of body force density, $\ddot{u}$ is the acceleration vector field, and x is a vector that represents the location of material points (particles) within the medium at time t. The key challenge in using equation (1) to model discontinuous system behaviour is the presence of the gradient operator, which implies the existence of the spatial derivative of the stress field and consequently the displacement field within the domain of interest. However, since these field variables are not continuous over features such as crack tip and crack surfaces, the derivatives in such instance are undefined. In the PD formulation, the equation of motion was casted such that the

integral operators replaced the derivatives on the right hand side of equation (1). A 'bond-based' PD equation of motion was originally proposed by [8] as

$$\rho(x)\ddot{u}(x,t) = \int_{\mathcal{H}_x} \mathrm{f}(u(q,t) - u(x,t), q - x)dV_q + b(x,t) \tag{2}$$

where u is the displacement vector field, $\mathcal{H}_x$ is the neighbourhood (horizon) of the particle located at point x. The pairwise force function f is the force per unit volume squared that a particle located at point q exerts on a particle located at point x.

If we assume a linear material behaviour, then the pairwise force function [8] takes the form

$$\mathrm{f}(\eta, \xi) = C(\xi)\eta \qquad \forall \xi, \eta \tag{3}$$

where $C(\xi)$ is a tensor valued function called the micromodulus function given by

$$C(\xi) = \frac{\partial \mathrm{f}(0, \xi)}{\partial \eta} \qquad \forall \xi \tag{4}$$

The PD equation of motion (2) therefore specialises to

$$\rho(x)\ddot{u}(x,t) = \int_{\mathcal{H}_x} C(x,q)\big(u(q,t) - u(x,t)\big)dV_k + b(x,t) \tag{5}$$

The discretised form of equation (5) as described in [13] is

$$\rho\ddot{u}_i^n = \sum_j^{N_i} C\big(x_j - x_i\big)\big(u_j - u_i\big)V_j + b_i^n \tag{6}$$

where N_i is the number of particles within the horizon of the particle located at x_i. The assembled PD equations of equilibrium for the body in matrix notation takes the form:

$$[M]\{\ddot{u}\} + [C]\{u\} = \{b\} \tag{7}$$

where $\{u\}$ is a vector of all displacement DoFs, $\{b\}$ is a vector that collect all applied body forces. [M] is a diagonal matrix of mass density, [C] is the micromodulus matrix which is analogous to the stiffness matrix in the FE method.

3.0 Static condensation

3.1 Reduced static peridynamic models

Consider a linear PD body $\mathcal{B}$ that is discretised into N number of material points. Considering static response, then the equation of motion (7) for a system of N material points is:

$$[C]_{N \times N}\{u\}_N = \{b\}_N \qquad (8)$$

The objective is to replace this system with a reduced degree of freedom system while maintaining the kinematic characteristics of the original system. Let $\{u_a\} \subset \{u\}_N$ be the primary (active) DoFs to be retained and $\{u_d\} \subset \{u\}_N$ be the secondary DoFs to be condensed out.

In order to carry out the condensation process, the assembled PD equilibrium equations are partitioned as follows:

$$\begin{bmatrix} [C_{aa}] & [C_{ad}] \\ [C_{da}] & [C_{dd}] \end{bmatrix} \begin{Bmatrix} \{u_a\} \\ \{u_d\} \end{Bmatrix} = \begin{Bmatrix} \{b_a\} \\ \{b_d\} \end{Bmatrix} \qquad (9)$$

The global vector of DoFs of the system may be written as

$$\{u\}_N = \{u\} = \begin{Bmatrix} \{u_a\} \\ \{u_d\} \end{Bmatrix} \qquad (10)$$

Multiplying out equation (9) we have

$$[C_{aa}]\{u_a\} + [C_{ad}]\{u_d\} = \{b_a\} \qquad (11)$$

$$[C_{da}]\{u_a\} + [C_{dd}]\{u_d\} = \{b_d\} \qquad (12)$$

Consider the solution to equation (12). If $[C_{dd}]$ is non singular, then we can solve for the DoFs to be condensed out:

$$\{u_d\} = [C_{dd}]^{-1}(\{b_d\} - [C_{ad}]\{u_a\}) \qquad (13)$$

Substituting equation (13) into equation (11) yields

$$[C_G]\{u_a\} = \{b_G\} \qquad (14)$$

Equation (14) is the condensed linearized PD equilibrium equation, where

$$[C_G] = [C_{aa}] - [C_{ad}][C_{dd}]^{-1}[C_{da}], \qquad \{b_G\} = \{b_a\} - [C_{ad}][C_{dd}]^{-1}\{b_d\} \qquad (15)$$

are the condensed micromodulus matrix and body force vector respectively. If we assume the inertia contribution as well as the external forces acting on the secondary DoFs to be negligible, this will permit a static relationship between the primary DoFs and the secondary DoFs such that equation (12) yields

$$\{u_d\} = [R_G]\{u_a\} \tag{16}$$

where $[R_G] \in R^{d \times a}$ represents the Guyan condensation matrix which is defined as

$$[R_G] = -[C_{dd}]^{-1}[C_{da}] \tag{17}$$

Introducing equation (17) into equation (10) gives the expression

$$\{u\} = [T_G]\{u_a\} \tag{18}$$

In equation (18), $[T_G] \in R^{n \times a}$ is a linear transformation matrix that maps DoFs in the reduced model onto DoFs in the full model and is defined as:

$$[T_G] = \begin{bmatrix} [I] \\ [R_G] \end{bmatrix} \tag{19}$$

Where $[I]$ is an $a \times a$ identity matrix. It is easily verifiable that equation (15) can be expressed as:

$$[C_G] = [T_G]^T [C][T_G], \qquad \{b_G\} = [T_G]^T \{b\} \tag{20}$$

Note that the static condensation is so called because we ignored the inertia effect on the deleted DoFs. Also note that in order to obtain the expression for the transformation matrix in equation (19), an assumption of zero body force density acting on the deleted DoFs was made. However, the fact that the expansion of equation (20) exactly gives the expression in equation (15) shows that this assumption does not affect the reduced stiffness matrix and the reduced force density vector. The condensed PD equilibrium equations as represented by equation (14) yields the exact solution of the PD model at the retained material points as would be obtained if we used the detailed model.

3.2   Reduced dynamic models

In order to reduce the order of a dynamic PD model, the equation of motion given in equation (7) may be written in partitioned form:

$$\begin{bmatrix} [M_{aa}] & [M_{ad}] \\ [M_{da}] & [M_{dd}] \end{bmatrix} \begin{Bmatrix} \{\ddot{u}_a\} \\ \{\ddot{u}_d\} \end{Bmatrix} + \begin{bmatrix} [C_{aa}] & [C_{ad}] \\ [C_{da}] & [C_{dd}] \end{bmatrix} \begin{Bmatrix} \{u_a\} \\ \{u_d\} \end{Bmatrix} = \begin{Bmatrix} \{b_a\} \\ \{b_a\} \end{Bmatrix} \tag{21}$$

If we assume the micromodulus function $[C]$ to be time invariant, then $[T_G]$ is independent of time and hence the second derivative of equation (18) with respect to time yields

$$\{\ddot{u}\} = [T_G]\{\ddot{u}_a\} \tag{22}$$

Introducing equations (18) and (22) into equation (7) and pre-multiplying both sides by the transpose of the transformation matrix $[T_G]$ gives the equation of equilibrium of the reduced model:

$$[M_G]\{\ddot{u}_a\} + [C_G]\{u_a\} = \{b_G\} \tag{23}$$

where the matrices $[M_G]$ and $[C_G]$ and the vector $\{b_G\}$ are the condensed mass matrix, condensed micromodulus matrix and condensed body force vector respectively associated with the reduced model, defined as:

$$[M_G] = [T_G]^T[M][T_G], \qquad [C_G] = [T_G]^T[C][T_G], \qquad \{b_G\} = [T_G]^T\{b\} \tag{24}$$

If we neglect dynamic effects in the reduced model, equation (23) specialises to the reduced model for static problem defined in equation (14). Since the majority of storage requirement and computational effort required to implement this condensation technique is used in the computation of $[C_{dd}]^{-1}$, a computationally more efficient way to achieve the condensation of the PD static model is to employ the standard Gauss-Jordan elimination procedure [20].

3.3 Reduced eigenvalue models

Assume that the solution u to equation (5) is given by the general form of a plane wave:

$$u(x,t) = Ae^{i(kx - \omega t)} \tag{25}$$

where u is the displacement of a point x, A is the constant amplitude vector, k is the wave number, ω is the wave frequency and t is time. Substituting equation (25) into equation (5) and assuming no body force applied will yield

$$-\omega^2 \rho(x)A = \int_{\mathcal{H}_x} C(x,q)\left(e^{ik(q-x)} - 1\right)dV_k \cdot A \tag{26}$$

Taking Euler's transformation of equation (26) gives

$$-\omega^2 \rho(x)u(x,t) = \int_{\mathcal{H}_x} C(x,q)\left(\cos\big(k(q-x)\big) + i\sin\big(k(q-x)\big) - 1\right)dV_k \cdot u(x,t) \tag{27}$$

Since the micromodulus function is an even function and $\sin\big(k(q-x)\big)$ is an odd function, equation (27) reduces to

$$\omega^2 \rho(x)A = \int_{\mathcal{H}_x} C(x,q)\big(1 - \cos\big(k(q-x)\big)\big)dV_k \cdot A \tag{28}$$

It can be inferred from equation (4) that the integral in equation (28) can be written in a matrix form. Using the simplified notation

$$\mathcal{D}(k,\xi) = \int_{\mathcal{H}_x} C(x,q)\big(1 - \cos\big(k(q-x)\big)\big)dV_k \tag{29}$$

with the definition that $\xi = q - x$, then equation (29) can be written as

$$\omega^2 \rho(x)A = \mathcal{D}(k,\xi) \cdot A \tag{30}$$

which gives us a classical eigenvalue problem with the following characteristic equation.

$$|\mathcal{D}(k,\xi) - \omega^2 \rho(x)| = 0 \tag{31}$$

The dispersion matrix $\mathcal{D}(k,\xi)$ first appeared in [8]. The eigenvalues and eigenvectors resulting from equation (31) gives the natural frequencies and natural modes of the peridynamic system. Equation (31) may be written in matrix form as

$$|[\mathcal{D}] - \omega^2[M]| = 0 \tag{32}$$

In equation (32), $[M] = \rho[I]$ is the mass-density matrix and $[I]$ is the identity matrix. The reduced order eigenvalue problem may be stated as

$$|[\mathcal{D}_G] - \omega^2[M_G]| = 0 \tag{33}$$

where $[\mathcal{D}_G]$ is the statically condensed dispersion matrix, and is defined as

$$[\mathcal{D}_G] = [T_G]^T[\mathcal{D}][T_G] \tag{34}$$

4.0 Condensation of the micromodulus function

This section will illustrate the typical form of a condensed micromodulus function. Consider a one-dimensional homogeneous bar of length 1.0 with a micromodulus function of the form:

$$C(\xi) = \begin{cases} 1.0\left(1 - \dfrac{|\xi|}{\delta}\right), & \text{if } |\xi| \leq \delta \\[2mm] 0, & \text{if } |\xi| > \delta \end{cases} \tag{35}$$

The bar is discretised into 100 nodes with interaction distance of $3dx$, where dx represents the distance between successive nodes. The reduced model consists of every fourth node in the detailed model as shown in Figure 1 in which retained nodes are designated with letter 'a' and deleted nodes are designated with letter 'd'.
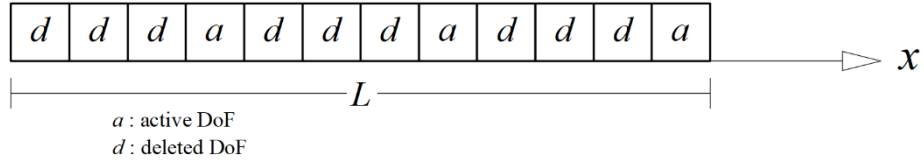
8

a : active DoF
d : deleted DoF

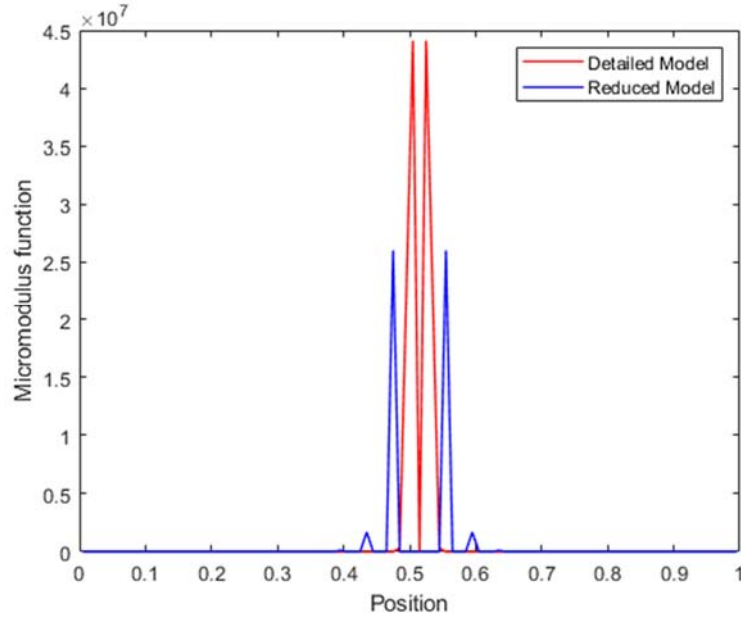**Figure 1.** Schematic representation of 1D reduction process

Figure 2. Coarsening of 1D Micromodulus function

The micromodulus of the detailed model and that of the reduced model is shown in Figure 2. The micromodulus function of the reduced model as can be seen from Figure 2 is defined only at the retained DoFs.

5.0 Numerical results

5.1   Reduction of static problems

In this section, a series of numerical experiments will be undertaken to illustrate the application of this model reduction technique in coarsening one and two-dimensional PD models.

5.1.1   A bar with periodic microstructure

Consider a composite bar with a length of 1.0 and a periodic microstructure consisting of alternate strips S_{hard} and S_{soft} of hard and soft materials, respectively, as shown in Figure 3. Each strip is 0.05 in length. The interaction distance, δ in both hard and soft materials is $3dx$. The micromodulus of the composite system is:

$$
C(\xi) = \begin{cases} 10.0\left(1 - \dfrac{|\xi|}{\delta}\right), & \text{if } |q - x| \leq \delta \text{ and } (x \in S_{\text{hard}} \text{ and } q \in S_{\text{hard}}) \\[4mm] 1.0\left(1 - \dfrac{|\xi|}{\delta}\right), & \text{if } |q - x| \leq \delta \text{ and } (x \in S_{\text{soft}} \text{ or } q \in S_{\text{soft}}) \\[4mm] 0, & \text{otherwise} \end{cases} \tag{36}
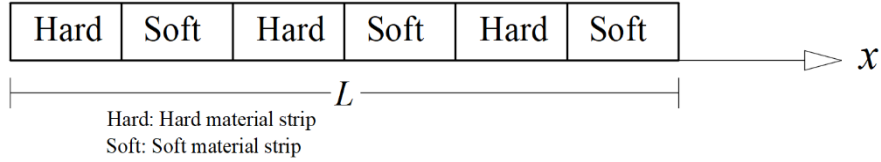$$

Figure 3. A schematic representation of the composite bar showing hard and soft material strips

Bonds with both ends in a hard strip are assigned hard material properties, otherwise, they are given soft material properties. Coarsening the detailed model is schematical represented by Figure 1. Every fourth material point in the detailed model is retained as an active point in the coarsened model. In the detailed model, a force density of $b = 0.002$ is applied to the rightmost material point while the leftmost material point is constrained from movement. Figure 4 shows the displacement fields of the detailed as well as coarsened model.
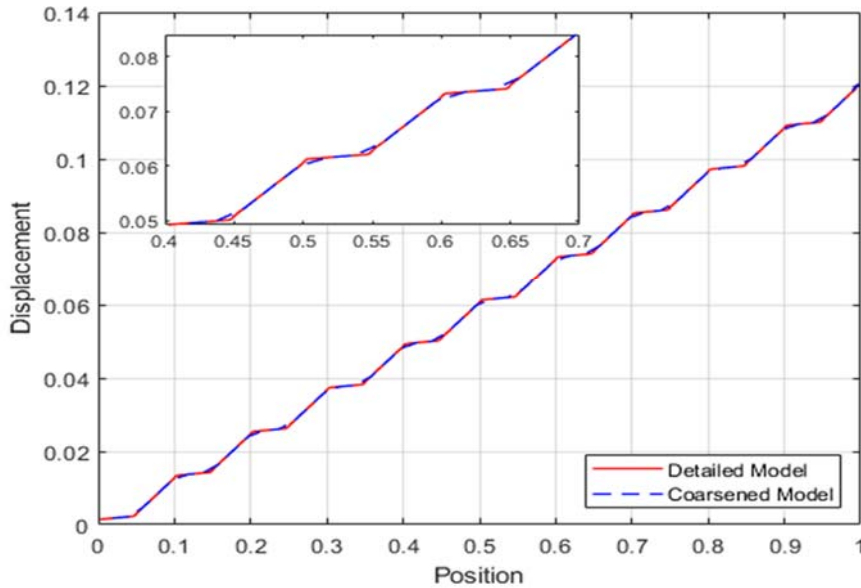
Figure 4. Displacement fields for detailed and reduced models

Results of displacement fields from simulation of both the detailed and reduced models shows exact match for all shared material points between the two models and hence both have the same global

stretch. However, as expected, the reduced model reflects less resolution of microstructural information than the detailed model.

5.1.2 Reduction of peridynamic plate static model

The static condensation can be employed in the reduction of static models of PD plates. The motivation for this may arises from the need to analyse a very large DoFs model and if the key focus is in determining the global response of the system without the need for a very detailed model. The objective in this example is to employ static condensation to eliminate all DoFs except those corresponding to the nodes located at the vertices of the plate shown in Figure 5. The bottom length of the plate is 1.0 while all other edge of the plate are of length 0.5. The micromodulus function of the plate material has the form

$$C(\xi) = 10.0\left(1 - \frac{|\xi|}{\delta}\right), \qquad \text{if} \ \ |q - x| \le \delta \tag{37}$$

The maximum interaction distance $\delta = 3dx$, where dx is the horizontal distance between nodes. A body force density of 0.001 is applied to the boundary nodes at topmost edge of the plate as shown in Figure 5. The detailed model is discretized into 100 material points.
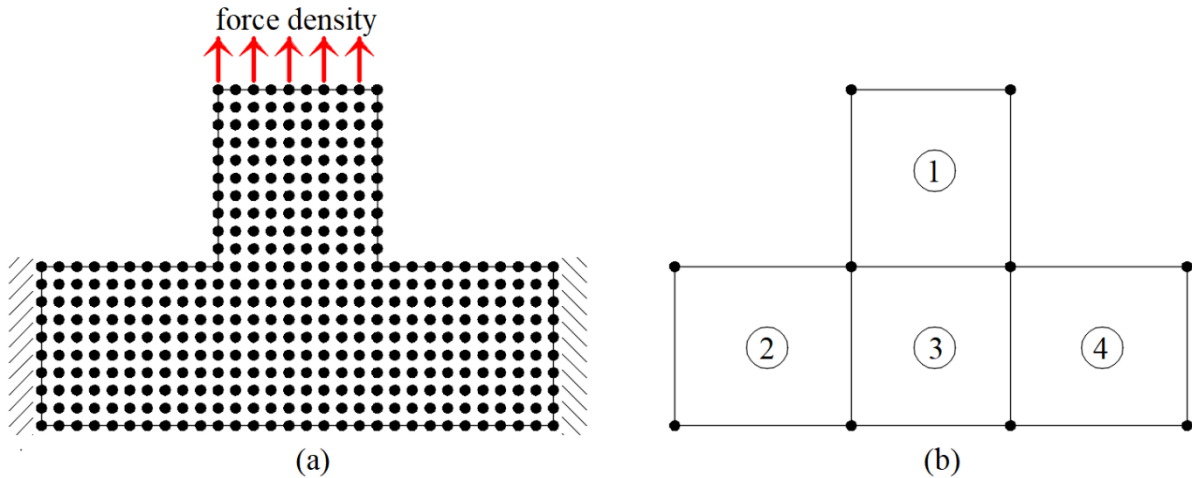

Figure 5. Schematic representation of the PD model of plate for static response analysis

The reduction procedure is achieved by condensing a group of nodes to form a substructure. At the end of the procedure, we are left with four (4) substructures bounded by ten (10) 'supernodes' as shown in Figure 5(b). Displacement results from analysis of both detailed and condensed models gives solutions that are exact.
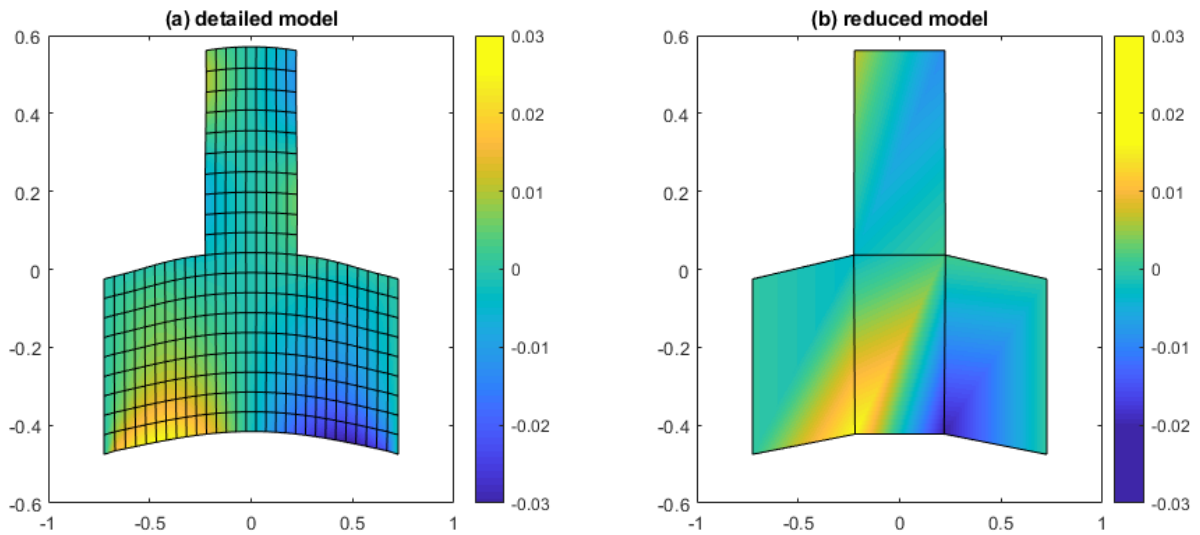
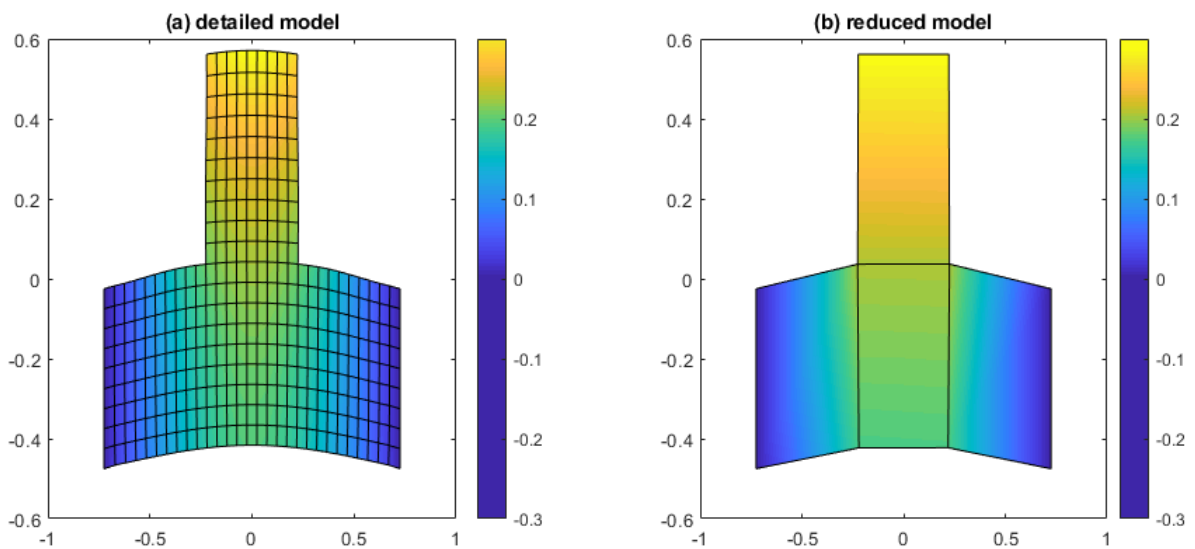**Figure 6.** Displacement profile in x-direction (a) Detail model (b) Condensed model

Figure 7. Displacement profile in y-direction (a) Detail model (b) Condensed model

5.2   Reduced Eigenproblems

5.2.1   A bar with one end fixed and the other free

Consider a bar of length $L = 1$ and uniform cross-sectional area $A = 1$ with the following material properties: Young Modulus $E = 1$, density $\rho = 1$. Let the bar be fixed at one end and free at the other end as shown in Figure 8.
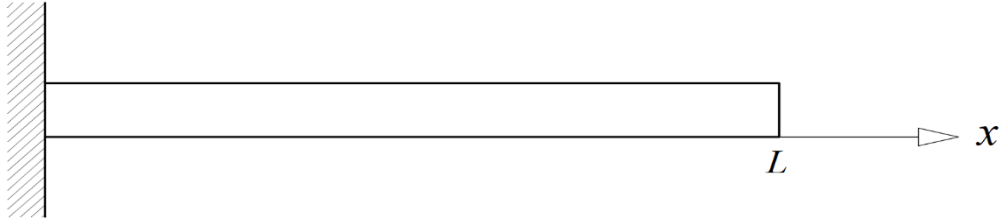
Figure 8. A bar with one end fixed and one end free

In order to numerically compute the natural frequencies and mode shapes arising from equation (33), the given bar is discretized into 1000 nodes. The interaction distance characteristic of the bar material, δ is assumed to be $3dx$, with dx being the distance between nodes. The material is assumed to have a micromodulus function of the form:

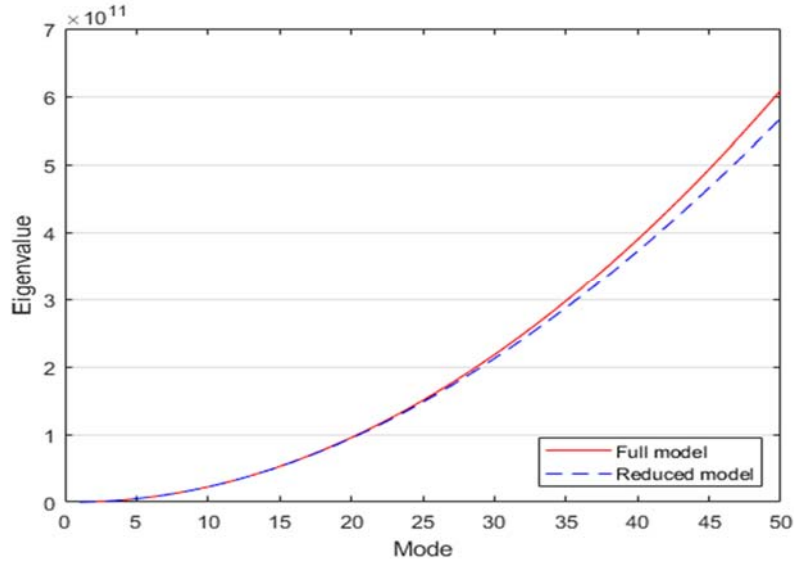$$C(\xi) = \frac{2E}{A\delta^2 |\xi|} \tag{38}$$

Figure 9. Comparison of eigenvalues from the full PD model and reduced model

The first five lowest frequencies of the bar as computed from equation (31) are shown in Table 1. These frequencies are then validated against frequencies obtained from the characteristic equation of the corresponding Finite Element (FE) model of the bar. The eigen values of the first 50 modes are presented in Figure 9.

Table 1. Natural frequencies of the first five modes computed using the full PD model, reduced PD model and FE analysis

Mode	FEM	Peridynamics		Difference between full and reduced model (%)
		Full model	Reduced model	
1	1.571	1.569	1.569	0.0006
2	4.712	4.708	4.708	0.0156
3	7.854	7.846	7.845	0.0724

13

4	10.996	10.984	10.982	0.1987
5	14.137	14.123	14.118	0.4223

Percentage difference between the natural frequencies computed from modal analysis of the full PD model and the reduced order PD model as presented in Table 1 shows a difference that ranges from 0.0006% to 0.4223%. This error margin coupled with the result presented in Figure 9 shows that the reduced model can accurately reproduce the lower eigenproperties of the full model.

5.3   Reduction of dynamic problems

In this section, the static condensation technique will be applied to reduce the order of a PD model and determine its time-history response. The objective is to determine the effectiveness of the model reduction technique in predicting the dynamic response of a given model despite the use of fewer DoFs. To illustrate the capabilities and limitation of the dynamic condensation technique, the bar shown in Figure 8 will be subjected to various excitation to determine the accuracy of the dynamic response predicted from the reduced order model. The bar will be assumed to have a Young modulus of 200GPa and a density of $7850 Kg/m^3$. The numerical integration method used to integrate the discretised peridynamic equation of motion for the transient analysis is the forward Euler method.

5.3.1   Free vibration of a peridynamic bar

The transient response of the PD bar will be studied. Three initial condition cases will be considered.

5.3.1.1   Case 1: Displacement induced initial excitation.

In this scenario, the bar is given an initial constant strain of 0.0001. The excitation is immediately removed to allow for free vibration of the bar. A transient analysis of the full PD model of the bar was conducted. The condensation process proceeded by retaining every forth node of the full PD model as shown in Figure 10.
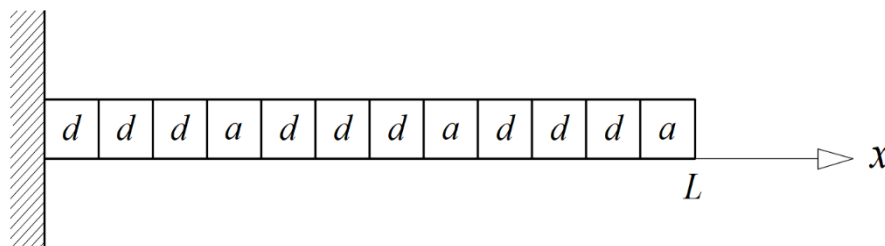

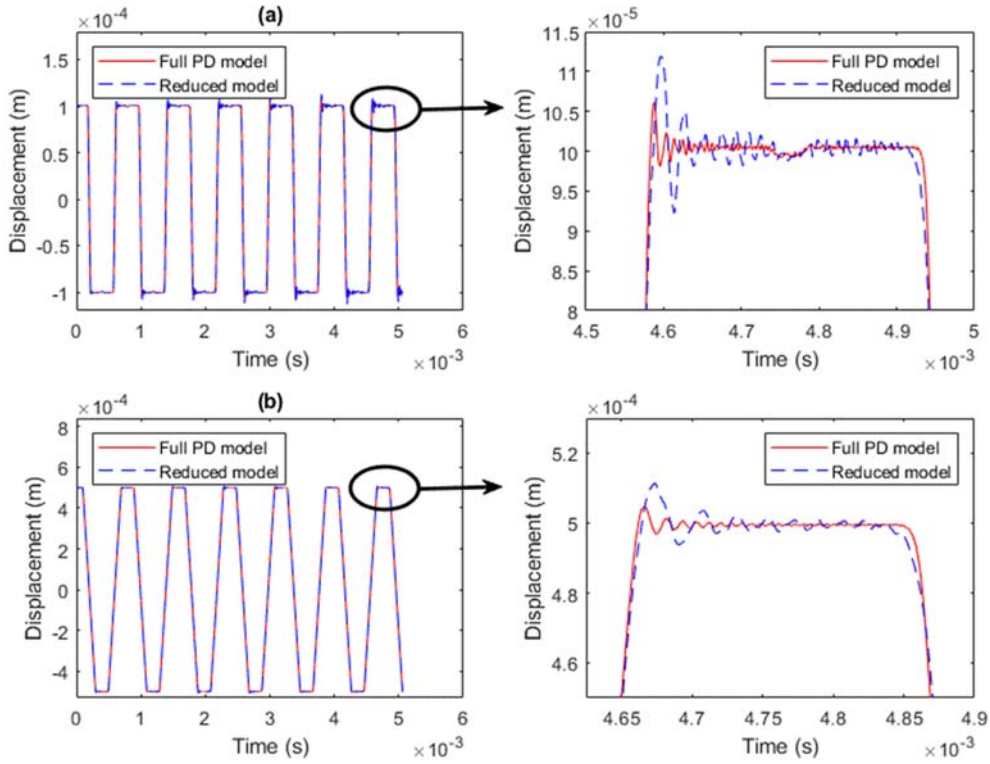**Figure 10.** Discretization and condensation of the full PD model

Figure 11. Time-history response of material points located at (a) x=0.0995, and (b) x=0.4995, for both full and reduced models
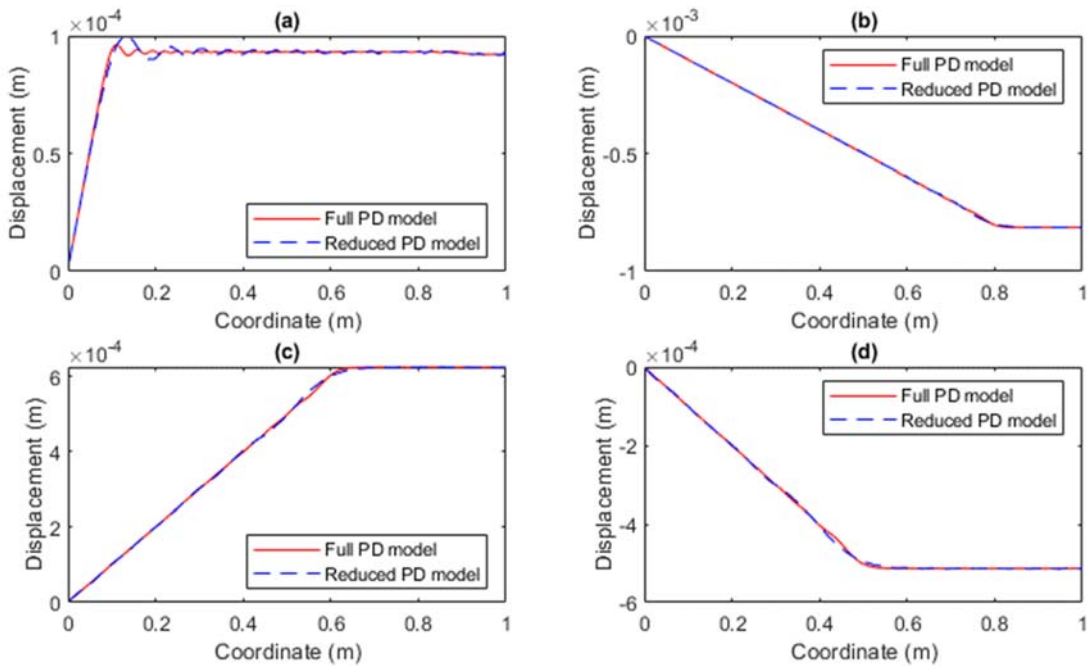

Figure 12. Displacement values at all nodes at (a) 5000th time step, (b) 10000th time step, (c) 20000th time step, and (d) 26000th time step

The results of the time-history response of material points located at $x = 0.0995$ and $x = 0.4995$ arising from both the full PD model and the reduced model are shown in Figure 11(a and b) respectively. Figure 12 shows the displacement values of all nodes at the 5000th, 10000th, 20000th and 26000th time

steps. These results show that the reduced model closely reproduces the dynamic response of the original PD model. However, as can be seen from Figure 11, there are some errors which arises because of neglecting inertia effects at the deleted DoF.

5.3.1.2 Case 2: Force induced initial excitation.

In this case study, initial constant body force density of $1 \times 10^4 \text{kN/m}^3$ is applied to every second node of the discretised PD bar and the force is immediately removed to allow for a free vibration of the bar. Equation (24) is used to condense the mass matrix, stiffness matrix and the force vector. The time-history response of points located at $x = 0.0995$, $x = 0.2995$, $x = 0.4995$ and $x = 0.7995$ for both the full and reduced models are shown in Figure 13 while Figure 14 shows the displacement values for all nodes at time steps 5000, 10000, 20000 and 26000. The results of the time-history analysis of the both the full PD model and the reduced model show that the condensation technique can accurately reproduce the dynamic response of the full PD model of the bar.
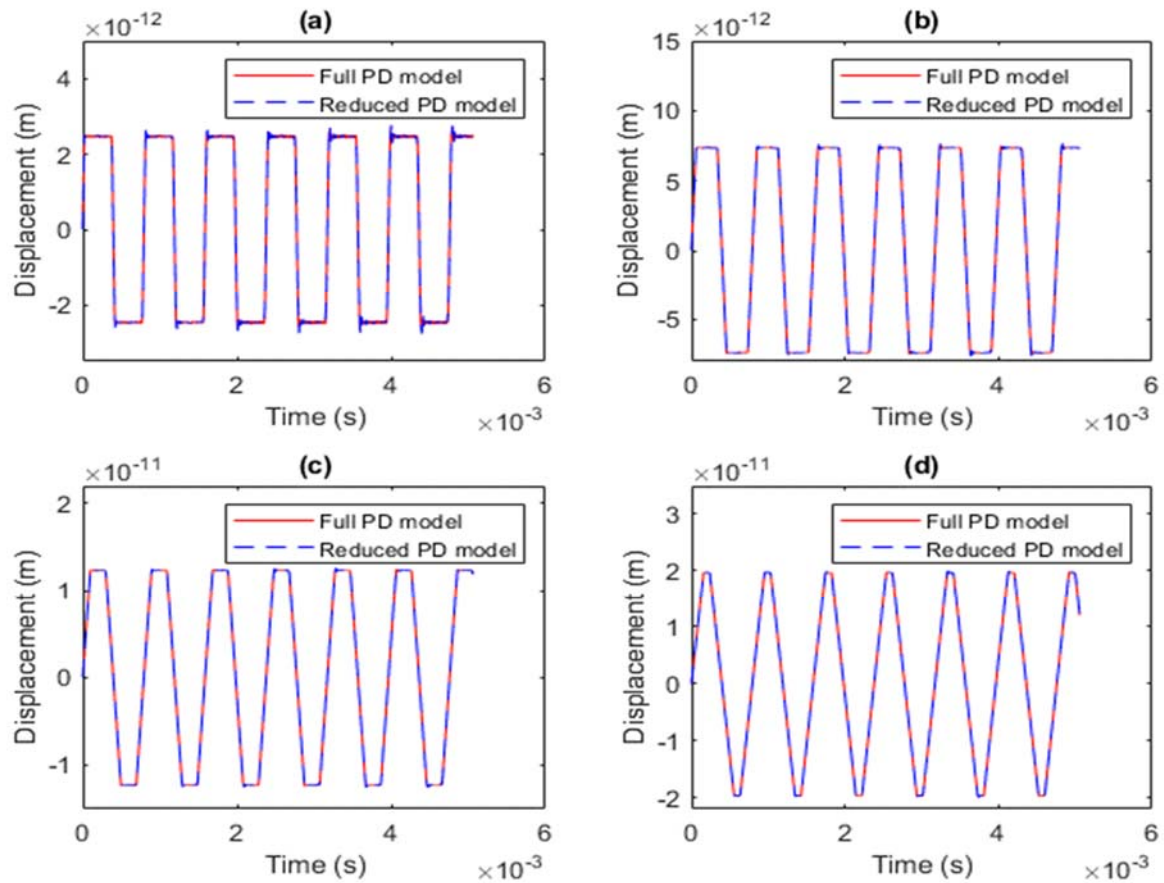

Figure 13. Time-history response of material points located at (a) x=0.0995 (b) x=0.2995 (c) x=0.4995 and (d) x=0.7995 for both the Full PD model and Condensed model

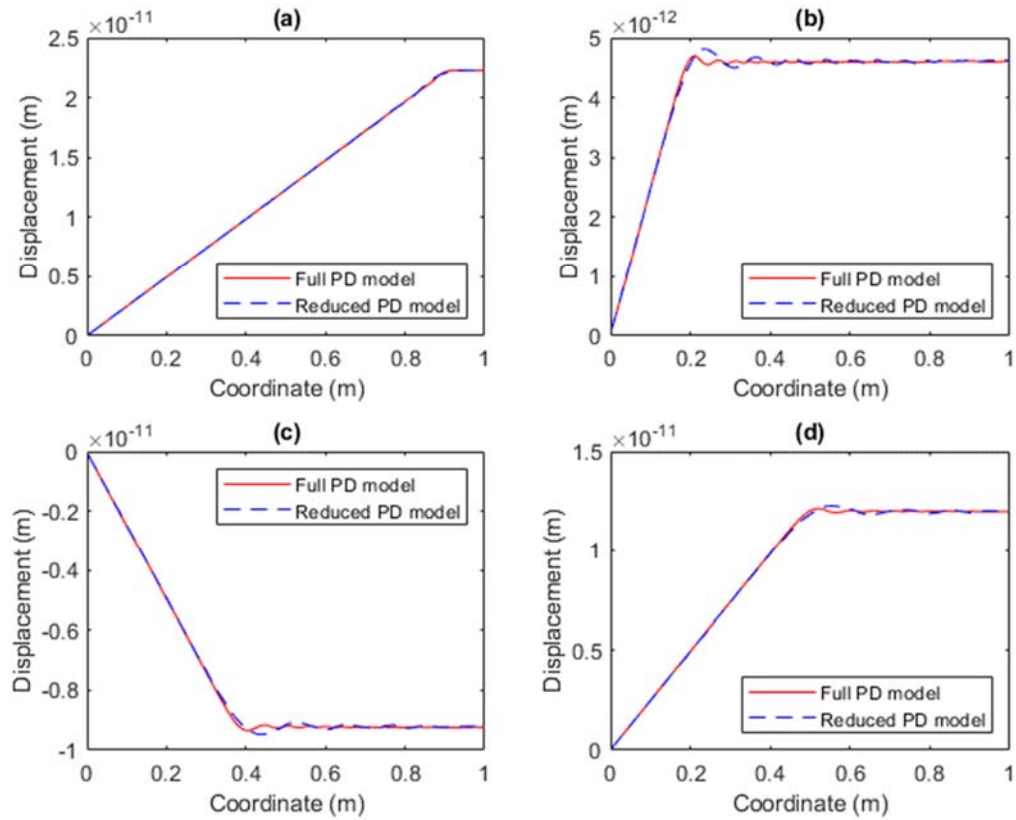**Figure 14.** Displacement values at all nodes at (a) 5000th time step, (b) 10000th time step, (c) 20000th time step, and (d) 26000th time step

5.3.2 Forced vibration

The bar in this case is assumed to be subjected to a time-dependent body force density of the form $\{b(t)\} = \{b_o\} \sin(\omega t)$ such that b_o is the amplitude of excitation, ω is the frequency of excitation. The force is applied at the rightmost node of the bar.
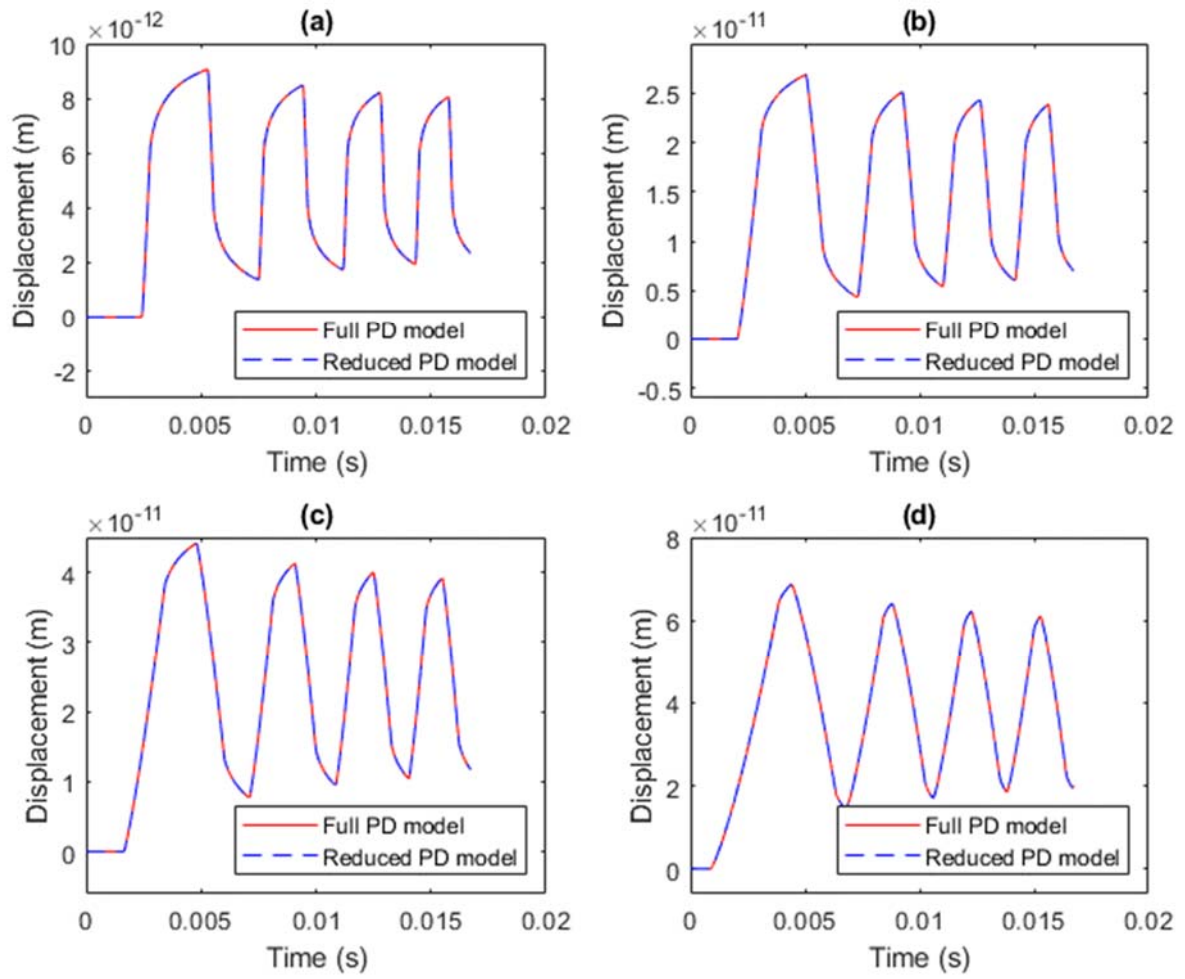
Figure 15. Time-history response of material points located at x=0.0995,0.2995,0.4995 and 0.7995 for both the Full PD model and Condensed model
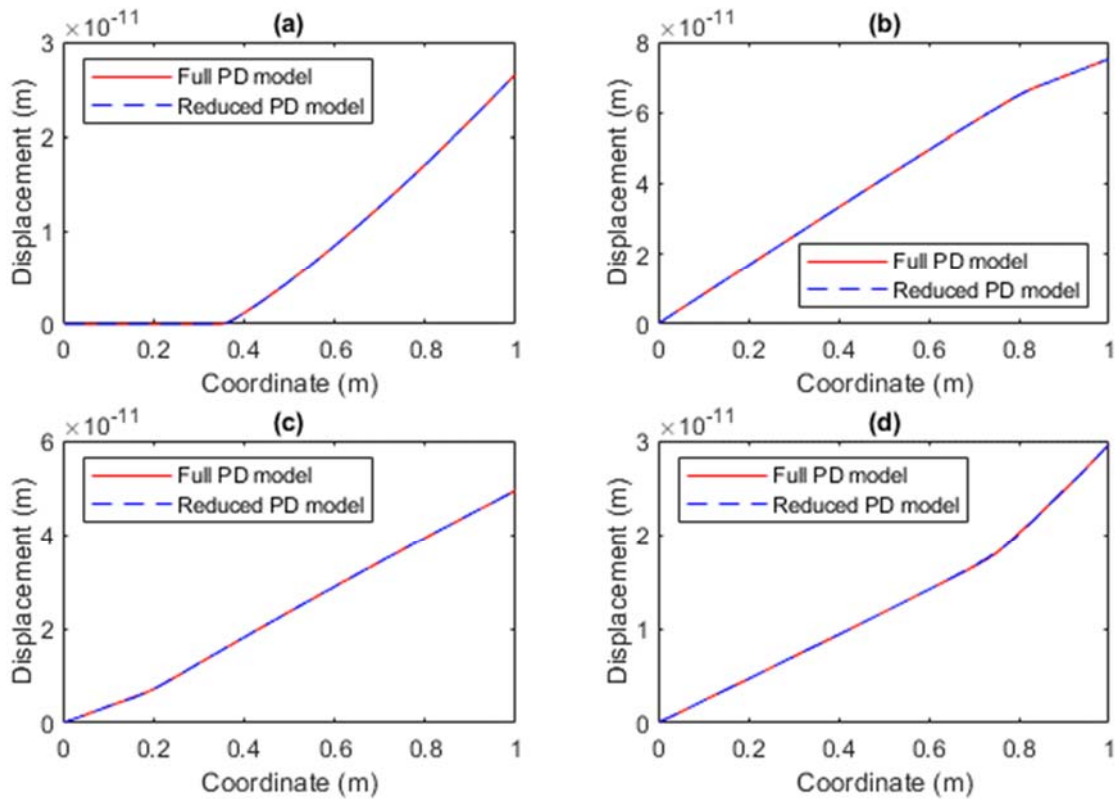
Figure 16. Displacement values at all nodes at (a) 10000th time step, (b) 20000th time step, (c) 50000th time step, and (d) 86000th time step

Results from a transient analysis of the full and reduced models for $b_o = 1 \times 10^4 kN/m^3$ and $\omega = 5 rad/sec$ for a total of 86,000 time steps are shown in Figure 15 and Figure 16. The dynamic response of the full PD model was accurately predicted using the reduced model.

6.0 Conclusion

A model reduction procedure for PD systems based on static condensation has been developed and investigated in this study. The results of numerical experiments presented shows that the reduction algorithm based on static condensation technique can closely preserve the characteristics and response of the original model. In the static regime, the algorithm has proved to yield identical results compared to those obtained from the original model. Although the results of the eigenresponse prediction of the reduced model shows some errors as shown in the eigenresponse and transient analysis, however, the results show that the proposed algorithm has capabilities of accurate prediction of dynamic response at low frequencies.

7.0 References

1. Wagih, A.M., M.M. Hegaze, and M.A. Kamel, *Satellite FE Model Validation for Coupled Load Analysis using Conventional and Enhanced Correlation Criteria*.

2. Guyan, R.J., *Reduction of stiffness and mass matrices.* AIAA Journal, 1965. **3**(2): p. 380-380.

3. Kidder, R.L., *Reduction of structural frequency equations.* 1984. **11**(6): p. 892-892.

4. Bourquin, F., *Component mode synthesis and eigenvalues of second order operators : discretization and algorithm.* ESAIM: M2AN, 1992. **26**(3): p. 385-423.

5. Bouhaddi, N. and R. Fillod, *Substructuring by a two level dynamic condensation method.* Computers & Structures, 1996. **60**(3): p. 403-409.

6. Pazs, M., *Dynamic Condensation.* AIAA Journal, 1984. **22**(5): p. 724-727.

7. Lin, R. and Y. Xia, *A new eigensolution of structures via dynamic condensation.* Journal of Sound and Vibration, 2003. **266**(1): p. 93-106.

8. Silling, S.A., *Reformulation of elasticity theory for discontinuities and long-range forces.* Journal of the Mechanics and Physics of Solids, 2000. **48**(1): p. 175-209.

9. Xia, W., et al., *Representative volume element homogenization of a composite material by using bond-based peridynamics.* Journal of Composites and Biodegradable Polymers, 2019.

10. Kefal, A. and E. Oterkus, *Displacement and stress monitoring of a chemical tanker based on inverse finite element method.* Ocean Engineering, 2016. **112**: p. 33-46.

11. Huang, Y., et al., *Peridynamic model for visco-hyperelastic material deformation in different strain rates.* Continuum Mechanics and Thermodynamics, 2019.

12. Nguyen, C.T. and S. Oterkus, *Peridynamics formulation for beam structures to predict damage in offshore structures.* Ocean Engineering, 2019. **173**: p. 244-267.

13. Silling, S.A. and E. Askari, *A meshfree method based on the peridynamic model of solid mechanics.* Computers & Structures, 2005. **83**(17): p. 1526-1535.

14. Yang, Z., et al., *A Kirchhoff plate formulation in a state-based peridynamic framework.* Mathematics and Mechanics of Solids, 2019: p. 108128651988752.

15. Agwai, A., I. Guven, and E. Madenci, *Predicting crack propagation with peridynamics: a comparative study.* International Journal of Fracture, 2011. **171**(1): p. 65.

16. Bobaru, F. and Y.D. Ha, *Adaptive Refinement and Multiscale Modeling In 2-D Peridynamics.* 2011. **9**(6): p. 635-660.

17. RAHMAN, R. and A. HAQUE, *A PERIDYNAMICS FORMULATION BASED HIERARCHICAL MULTISCALE MODELING APPROACH BETWEEN CONTINUUM SCALE AND ATOMISTIC SCALE.* International Journal of Computational Materials Science and Engineering, 2012. **01**(03): p. 1250029.

18. Silling, S.A., *A Coarsening Method for Linear Peridynamics.* 2011. **9**(6): p. 609-622.

19. Galadima, Y., E. Oterkus, and S. Oterkus, *Two-dimensional implementation of the coarsening method for linear peridynamics.* AIMS Material Science, 2019. **6**(2): p. 252-275.

20. Paz, M., *Practical Reduction of Structural Eigenproblems.* American Society Of Civil Engineers ASCE Journals, 1983. **109**(11): p. 2591-2599.